

*Regular article*

# Partial Hessian vibrational analysis: the localization of the molecular vibrational energy and entropy

Hui Li, Jan H. Jensen

Department of Chemistry, University of Iowa, Iowa City, IA 52242, USA

Received: 21 September 2001 / Accepted: 30 October 2001 / Published online: 22 March 2002  
© Springer-Verlag 2002

**Abstract.** The partial Hessian vibrational analysis (PHVA), in which only a subblock of the Hessian matrix is diagonalized to yield vibrational frequencies for partially optimized systems, is extended to the calculation of vibrational enthalpy and entropy changes for chemical reactions. The utility of this method is demonstrated for various deprotonation reactions by reproducing full HVA values to within 0.1–0.4 kcal/mol, depending on the number atoms included in the PHVA. When combined with the hybrid effective fragment potential method [Gordon MS, et al. (2001) *J Phys Chem A* 105:293–307], the PHVA method can provide (harmonic) free-energy changes for localized chemical reactions in very large systems.

**Key words:** Ab initio – Hessians – Vibrational analysis – Constrained optimizations – Quantum mechanics/molecular mechanics

## 1 Introduction

One of the most computationally demanding aspects of calculating a reaction free energy using electronic structure theory is the calculation of the vibrational energy and entropy contributions. The computational expense is incurred by the calculation of the matrix of second energy-derivatives (i.e. the Hessian or force constant matrix) which yields harmonic vibrational frequencies upon diagonalization. The analytic computation of the Hessian matrix requires the evaluation of about 9 times as many atomic orbital integrals compared to an energy evaluation, as well as a partial integral transformation (to solve the coupled-perturbed Hartree–Fock equations) that requires significant amounts of memory and disk space. The numerical (finite-difference) computation of the Hessian requires a minimum of

$3N + 1$  energy and gradient evaluations (where  $N$  is the number of atoms), and usually  $6N + 1$  energy and gradient evaluations for acceptable accuracy. Thus, the computation of the Hessian quickly becomes computationally intractable as the size of the system increases.

If only a single localized vibration is required, part of the potential-energy surface can be constructed by moving a selected atom or group of atoms and deriving the associated numerical force constant explicitly. This practice has been especially common in the study of the vibrational motion of adsorbates on surfaces. [1] For polyatomic adsorbates this method can be generalized by constructing and diagonalizing the appropriate subblock of the Hessian. This approach, referred to hereafter as the partial Hessian vibrational analysis (PHVA), has been popularized by Head [2] for the study of surface chemistry. However, whether the PHVA can also yield accurate vibrational enthalpy and entropy changes for chemical reactions has, to our knowledge, not been tested. This issue is addressed in this article, which is organized as follows.

First, we review the PHVA method, propose some modifications, and discuss some additional considerations related to the computation of the vibrational enthalpy and entropy. Second, we apply the method to proton transfer and abstraction reactions involving acetic acid,  $\alpha$ -amino tridecanoic acid, and the glycyl-ly-syl-glycine (GKG) tripeptide. The latter case presents an extension of the PHVA method to a hybrid quantum mechanical/molecular mechanical (QM/MM) description of a molecule. Finally, the results are summarized and future applications of the PHVA are discussed.

## 2 Theory

### 2.1 Review of full numerical Hessian computation and vibrational analysis

Consider a molecule, A, consisting of  $N$  atoms, each with nuclear charge  $Z_i$ , Cartesian coordinate  $q_i(0)$ , and mass  $m_i$ ,

$$A = \{Z_i, q_i(0), m_i\}, \quad i = 1, 2, 3, \dots, 3N. \quad (1)$$

Correspondence to: J.H. Jensen  
e-mail: jan-jensen@uiowa.edu

We assume that **A** is at a stationary point, so the energy gradients are zero,

$$g_i(0) = \left( \frac{\partial E}{\partial q_i} \right)_{q_i(0)} = 0 . \quad (2)$$

The matrix of energy second derivatives (the Hessian, **K**) can be computed numerically (in practice **K** is always symmetrized:  $K_{ij} = K_{ji} = (K_{ij} + K_{ji})/2$ ),

$$\begin{aligned} K_{ij} &= \left( \frac{\partial^2 E}{\partial q_i \partial q_j} \right)_{q_i(0)} \\ &\approx \left( \frac{g_i(+j) - g_i(-j)}{2dl} \right) \\ \text{or } &\approx \left( \frac{g_i(+j) - g_i(0)}{dl} \right) \end{aligned} \quad (3)$$

either by double or single displacement by an amount  $dl$  followed by a gradient evaluation:

$$g_i(\pm j) = \left( \frac{\partial E}{\partial q_i} \right)_{q_j=q_j(0) \pm dl}, \quad j = 1, 2, 3 \dots 3N . \quad (4)$$

The harmonic vibrational frequencies,  $\{v_i\}$ , of molecule **A** are obtained by

$$v_i = \left( \frac{\lambda_i^{1/2}}{2\pi} \right), \quad (5)$$

where  $\{\lambda_i\}$  are the eigenvalues of the mass-weighted Hessian (**K'**),

$$K'_{ij} = \frac{1}{\sqrt{m_i m_j}} K_{ij} . \quad (6)$$

For nonlinear (linear) molecules six (five) frequencies are zero, since they correspond to rigid rotation and translation of the entire molecule, motions for which the energy and gradient are invariant.

In practice, numerical inaccuracy leads to nonzero translational and rotational eigenvalues. These can be made identically zero by a projection,

$$\mathbf{K}^p = \mathbf{P} \mathbf{K}' \mathbf{P}^t, \quad (7)$$

where **P** is the projection matrix suggested by Miller et al. [3].

## 2.2 The PHVA

Head has proposed a strategy (the PHVA) by which only the frequencies of part of a chemical system are computed. For example, the molecule **A** considered earlier is divided into two regions, **B** and **C**, with  $n$  and  $N - n$  atoms, respectively:

$$\begin{aligned} \mathbf{A} &= \mathbf{B} + \mathbf{C}, \\ \mathbf{A} &= \{Z_i, q_i(0), m_i\}, \quad i = 1, 2, 3, \dots 3N, \\ \mathbf{B} &= \{Z_i, q_i(0), m_i\}, \quad i = 1, 2, 3, \dots 3n, \\ \mathbf{C} &= \{Z_i, q_i(0), m_i\}, \quad i = 3n + 1, 3n + 2, \dots 3N . \end{aligned} \quad (8)$$

In block form, the Hessian can thus be written as

$$\mathbf{K} = \begin{pmatrix} \mathbf{K}_{BB} & \mathbf{K}_{BC} \\ \mathbf{K}_{CB} & \mathbf{K}_{CC} \end{pmatrix} . \quad (9)$$

Head considered the case where region **B** is an adsorbate and region **C** is a surface and showed that diagonalization of only (mass-weighted)  $\mathbf{K}_{BB}$  yields reasonable frequencies for methoxy adsorption on Cu and Al surfaces by comparison with experiment [2]. The numerical double-difference computation of  $\mathbf{K}_{BB}$  only requires  $6n$  gradient evaluations, and since  $n < N$ , this approach results in significant savings of computer time compared to computing all the frequencies.

## 2.3 PHVA vibrational enthalpy and entropy changes

The results obtained by Head suggest that the PHVA method may provide computationally inexpensive enthalpy and entropy corrections to a reaction energy, provided the chemical change is localized (in region **B**).

Within the harmonic oscillator–rigid rotor approximation, the free energy of a molecule is given by the electronic energy ( $E$ ) plus translational, rotational, and vibrational enthalpy and entropy,

$$\begin{aligned} G &= E + G_{\text{trans}} + G_{\text{rot}} + G_{\text{vib}} \\ &= E + (H_{\text{trans}} - TS_{\text{trans}}) + (H_{\text{rot}} - TS_{\text{rot}}) + (H_{\text{vib}} - TS_{\text{vib}}) . \end{aligned} \quad (10)$$

In our approach  $G_{\text{trans}}$  and  $G_{\text{rot}}$  are calculated in the usual way for the entire molecule, in particular the total molecular mass and moments of inertia are used to compute  $S_{\text{trans}}$  and  $S_{\text{rot}}$ , respectively.

The vibrational enthalpy and entropy should reflect vibrational motion within **B** and motion of **B** relative to **C**. However, the  $3n$  vibrational modes resulting from the diagonalization of  $\mathbf{K}_{BB}$  also contain contributions from the overall rotation and translation of the molecule as well as the motion of **C** relative to **B**. Both issues can be most easily dealt with by constructing the following matrix,

$$\mathbf{K} = \begin{pmatrix} \mathbf{K}_{BB} & \mathbf{0} \\ \mathbf{0} & \mathbf{K}_{CC}^\varepsilon \end{pmatrix}, \text{ where } \mathbf{K}_{CC}^\varepsilon = \begin{pmatrix} \varepsilon & 0 & 0 \\ 0 & \ddots & 0 \\ 0 & 0 & \varepsilon \end{pmatrix} \varepsilon = 10^{-8} \text{ au} . \quad (11)$$

Conceptually, this corresponds to using near-infinite masses for the atoms in **C**. The value of  $\varepsilon$  is chosen to remove spurious imaginary frequencies from numerical errors due to the numerical second-derivative evaluation. Upon the usual projection (Eq. 7) and mass-weighting (Eq. 6), diagonalization yields (for nonlinear molecules)

1. Six zero eigenvalues with modes corresponding to translational and rotational motion of the entire molecule.
2.  $3(N - n) - 6$  small (less than  $1 \text{ cm}^{-1}$ ) eigenvalues with modes corresponding mainly to internal motion within region **C**.

- Three eigenvalues (typically less than  $10 \text{ cm}^{-1}$ ) with modes corresponding mainly to motion of region C relative to region B.
- $3n - 3$  eigenvalues with modes corresponding mainly to relative motion of B and C as well as internal motion within region B.

The vibrational energy of region B (with  $n$  atoms) is calculated by [4]

$$H_{\text{vib}} = R \sum_{i=1}^{3n-3} \left( \frac{h\nu_i^{\text{B}}}{2k_{\text{B}}} + \frac{h\nu_i^{\text{B}}}{k_{\text{B}}} \frac{1}{\exp(h\nu_i^{\text{B}}/k_{\text{B}}T) - 1} \right),$$

$$S_{\text{vib}} = R \sum_{i=1}^{3n-3} \left( \frac{h\nu_i^{\text{B}}}{k_{\text{B}}T} \frac{1}{\exp(h\nu_i^{\text{B}}/k_{\text{B}}T) - 1} - \ln[1 - \exp(h\nu_i^{\text{B}}/k_{\text{B}}T)] \right), \quad (12)$$

where  $\{\nu_i^{\text{B}}\}$  corresponds to the  $3n - 3$  largest eigenvalues (any imaginary frequencies will reduce this number further) described in point 4.

This method has been implemented in the June 25, 2001 version of the quantum chemistry program GAMESS, [5] which was used for all the calculations reported here.

### 3 Results and discussion

#### 3.1 Acetic acid

##### 3.1.1 Deprotonation

The methodology outlined in the previous section is demonstrated for the deprotonation of acetic acid at the AM1 level of theory (chosen for computational

convenience). The equilibrium geometries of  $\text{CH}_3\text{COOH}$  and  $\text{CH}_3\text{COO}^-$  were obtained using AM1, and the vibrational frequencies resulting from a vibrational analysis of the full Hessian (FHVA), calculated by double displacement and projected (Eq. 7), are listed in Table 1. The sums of the translation, rotational, and vibrational enthalpy ( $H_{\text{trv}}$ ) and free energy ( $G_{\text{trv}}$ ) for each molecule are listed in Table 2, as are the changes in these quantities on going from  $\text{CH}_3\text{COOH}$  to  $\text{CH}_3\text{COO}^-$  ( $\Delta H_{\text{trv}}$  and  $\Delta G_{\text{trv}}$ ).

Next we divide  $\text{CH}_3\text{—COOH}$  and  $\text{CH}_3\text{COO}^-$  at the CC bond, and compute the Hessians for only the COOH and  $\text{COO}^-$  groups. The frequencies resulting from this PHVA are listed in Table 1, along with the FHVA reference values for comparison.

First we compare the FHVA and PHVA frequencies for  $\text{CH}_3\text{COOH}$ . Since both Hessians are projected, diagonalization yields six zero eigenvalues with modes

**Table 2.** Thermodynamical translational plus rotational plus vibrational enthalpies ( $H_{\text{trv}}$ ) and free energies ( $G_{\text{trv}}$ ) of acetic acid (acid), acetate (base) and intramolecular proton transfer transition state (TS) computed by the PHVA and the FHVA. The thermodynamic energy changes for deprotonation ( $\Delta_{\text{base-acid}}$ ) and proton transfer ( $\Delta_{\text{TS-acid}}$ ) were calculated from both the PHVA and FHVA values, as were the errors of PHVA compared to FHVA ( $\Delta\Delta_{\text{PHVA-FHVA}}$ ). All values in kcal/mol

	PHVA		FHVA		$\Delta\Delta_{\text{PHVA-FHVA}}$	
	$H_{\text{trv}}$	$G_{\text{trv}}$	$H_{\text{trv}}$	$G_{\text{trv}}$	$\Delta\Delta H_{\text{trv}}$	$\Delta\Delta G_{\text{trv}}$
Acid	18.87	-0.99	42.52	21.88		
Base	11.28	-8.29	34.87	14.55		
TS	15.78	-3.83	39.38	18.92		
$\Delta_{\text{base-acid}}$	-7.59	-7.30	-7.65	-7.33	0.06	0.03
$\Delta_{\text{TS-acid}}$	-3.09	-2.84	-3.14	-2.96	0.05	0.12

**Table 1.** Restricted Hartree-Fock/AM1 frequencies ( $\text{cm}^{-1}$ ) calculated using the partial Hessian vibrational analysis (PHVA) for  $\text{CH}_3\text{COOH}$  and  $\text{CH}_3\text{COO}^-$  and their difference. Similar values calculated by a full Hessian vibrational analysis (FHVA) are given for comparison

Mode	PHVA			FHVA		
	$\text{CH}_3\text{COOH}$	$\text{CH}_3\text{COO}^-$	Difference	$\text{CH}_3\text{COOH}$	$\text{CH}_3\text{COO}^-$	Difference
1	0.00	0.00	0.00	0.00	0.00	0.00
2	0.00	0.00	0.00	0.00	0.00	0.00
3	0.00	0.00	0.00	0.00	0.00	0.00
4	0.00	0.00	0.00	0.00	0.00	0.00
5	0.00	0.00	0.00	0.00	0.00	0.00
6	0.00	0.00	0.00	0.00	0.00	0.00
7	0.51	0.46	0.05	1,364.08	1,388.57	-24.49
8	0.51	0.47	0.04	1,371.39	1,399.29	-27.90
9	0.46	0.47	-0.01	1,412.86	1,401.82	11.04
10	0.47	0.51	-0.04	3,057.82	3,071.74	-13.92
11	0.47	0.51	-0.04	3,068.47	3,077.94	-9.47
12	0.51	0.51	0.00	3,152.09	3,160.45	-8.36
13	4.08	2.72	1.36	62.52	65.55	-3.03
14	7.52	7.76	-0.24	1,039.40	1,029.72	9.68
15	9.82	8.98	0.84	1,073.79	1,041.55	32.24
16	208.43	212.82	-4.39	1,100.29	1,063.42	36.87
17	319.08	344.57	-25.49	418.88	453.42	-34.54
18	548.78		548.78	524.10		524.10
19	665.06	701.36	-36.30	592.60	591.87	0.73
20	757.22	787.65	-30.43	570.03	614.63	-44.60
21	1,420.20		1,420.20	1,430.25		1,430.25
22	1,517.04	1,657.29	-140.25	1,549.39	1,663.74	-114.35
23	2,077.02	2,044.77	32.25	2,088.16	2,050.01	38.15
24	3,431.14		3,431.14	3,431.18		3,431.18

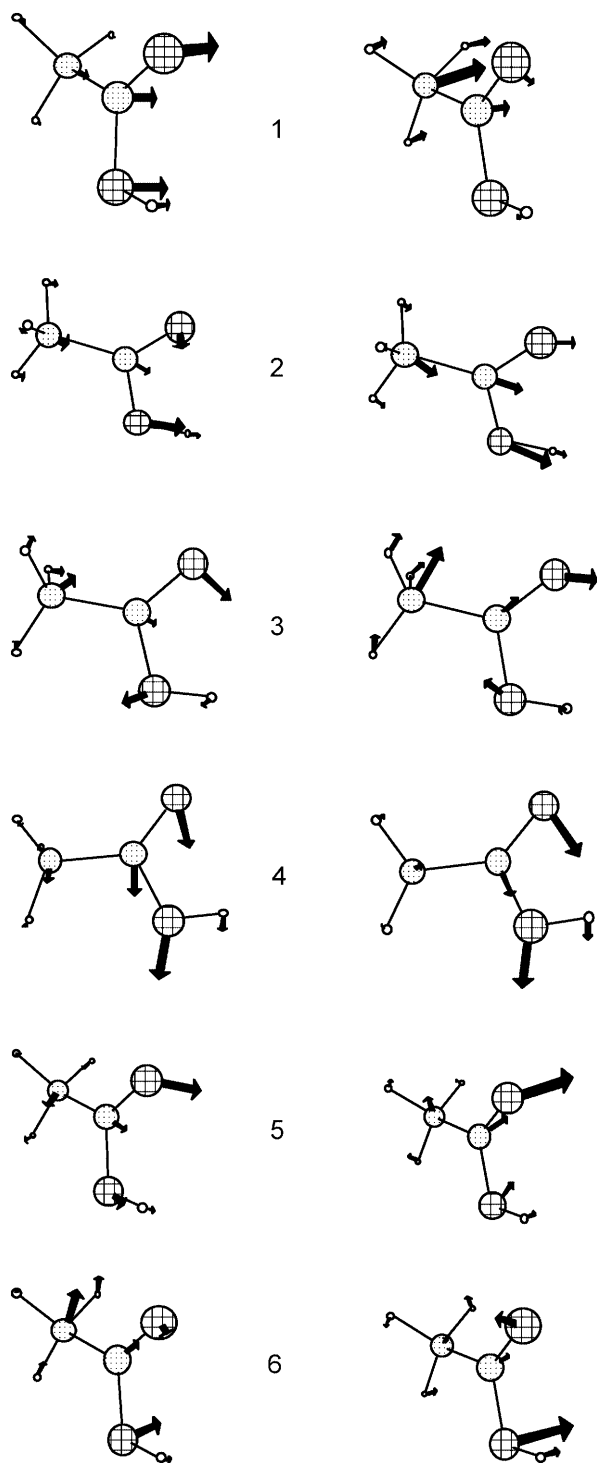


**Fig. 1.** The translational and rotational modes (modes 1–6 in Table 1) of acetic acid from a partial Hessian vibrational analysis (PHVA, left) and a full Hessian vibrational analysis (FHVA, right)

corresponding to translation and rotation (Fig. 1). The next six PHVA frequencies fall in the range  $0.47\text{--}0.51\text{ cm}^{-1}$  and correspond mainly to motion of the  $\text{CH}_3$  group (Fig. 2a). Very similar modes can be found in the FHVA (Fig. 2b), since they represent orthogonal complements to the  $\mathbf{K}_{\text{BB}}$  eigenvectors and the projection

operator. We note that these FHVA frequencies change by  $8\text{--}28\text{ cm}^{-1}$  on going to  $\text{CH}_3\text{COO}^-$ .<sup>1</sup> The next three PHVA frequencies fall in the range  $4.08\text{--}9.82\text{ cm}^{-1}$  and correspond mainly to motion of the  $\text{CH}_3$  group relative to the  $\text{COOH}$  group (Fig. 3a). Three similar modes (Fig. 3b) can be found in the FHVA and these corresponding FHVA frequencies change by  $3\text{--}32\text{ cm}^{-1}$  on going to  $\text{CH}_3\text{COO}^-$ . The last nine frequencies (Fig. 4a) fall in the range  $208.43\text{--}3,431.14\text{ cm}^{-1}$ . The low-frequency modes correspond in part to relative motion of the  $\text{CH}_3$  and  $\text{COOH}$  groups, while the high-frequency modes are almost independent of the  $\text{CH}_3$  group. The last nine FHVA frequencies are shown in Fig. 4b for comparison. Most interestingly, the frequencies that are lost upon deprotonation are generally well reproduced by the PHVA procedure (within  $0\text{--}25\text{ cm}^{-1}$  of the FHVA results), as are the changes in the remaining frequencies (the errors in the changes are within  $6\text{--}41\text{ cm}^{-1}$  of the FHVA results).

Of course, the resulting PHVA  $H_{\text{trv}}$  and  $G_{\text{trv}}$  for  $\text{CH}_3\text{COOH}$  and  $\text{CH}_3\text{COO}^-$  (Table 2) differ significantly from their FHVA counterparts; however, the changes in these values on going from  $\text{CH}_3\text{COOH}$  to  $\text{CH}_3\text{COO}^-$  ( $\Delta H_{\text{trv}}$  and  $\Delta G_{\text{trv}}$ ) are reproduced to within  $0.06\text{ kcal/mol}$ . The error is entirely due to the vibrational component, since the translational and rotational components are identical in the FHVA and PHVA approaches.

### 3.1.2 Proton transfer

The PHVA can be applied to transition states (TSs) as well. The FHVA imaginary frequency and the corresponding normal mode obtained for the proton-transfer TS within acetic acid are shown in Fig. 5a. The corresponding PHVA results, which are virtually identical to the FHVA results, are shown in Fig. 5b. Furthermore, the PHVA activation enthalpy and free energy are within  $0.12\text{ kcal/mol}$  of the FHVA results (Table 2).

### 3.2 $\alpha$ -Amino tridecanoic acid

Acetic acid was chosen as an initial test case because its small size allowed the comparison of all the normal modes in detail. However, in practice the PHVA analysis will be applied to much larger systems, where the error may increase owing to the increased number of low frequencies with delocalized modes. In order to address this point, we present the PHVA enthalpies and free energies for deprotonation and intramolecular proton transfer within  $\alpha$ -amino tridecanoic acid (Fig. 6) relative to their respective FHVA values as a function of the number of atoms included in the PHVA.

The results for the deprotonation energy (Fig. 7) show that the error has increased to  $0.1\text{--}0.2\text{ kcal/mol}$  for a PHVA including only the  $\text{COOH}$  group, compared to acetic acid; however, this is still a relatively small error compared to the typical error of a reaction energy rela-

<sup>1</sup>An error of  $1\text{ cm}^{-1}$  results in an error in the zero-point energy of  $0.0014\text{ kcal/mol}$ .

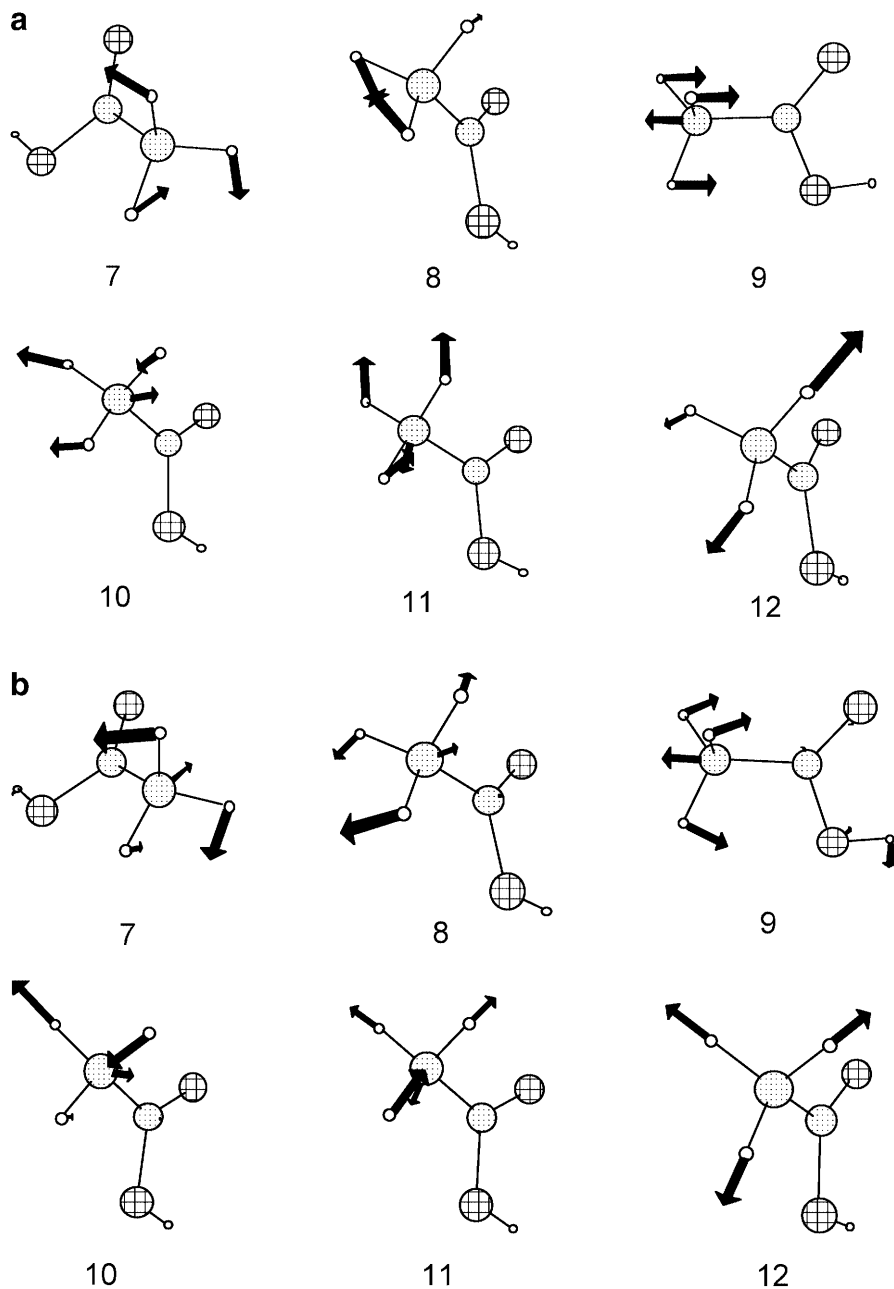


**Fig. 2.** **a** PHVA and **b** FHVA derived frequencies of acetic acid corresponding mainly to internal motion of the CH<sub>3</sub> group (modes 7–12 in Table 1)

tive to experiment. The error tends to be slightly larger for the free energy compared to the enthalpy. As expected the absolute error decreases as more atoms are included in the PHVA.

A similar result is obtained for the proton-transfer activation energy (Fig. 8), although there is an initial increase in the free-energy error as more atoms are included in the PHVA. The cause of this 0.16-kcal/mol error increase is not clear, but can be eliminated by including more atoms in the PHVA.

In general, we have found that the boundary between atoms included in and excluded from the PHVA analysis should be separated from the reaction region by at least two bonds in order to obtain good enthalpies and free energies.

### 3.3 Application of the PHVA within the effective fragment potential method

As noted by Head, only the atom included in the PHVA need have zero first energy derivatives so that the PHVA can be used to obtain frequencies (and now the resulting enthalpy and free energy corrections) for partially optimized systems. Here, we pursue this issue within the context of the effective fragment potential (EFP) method [6], a hybrid *ab initio* QM/MM method. An EFP represents the molecular electrostatic potential by a distributed multipole expansion [7] (charges through octupoles at all atomic centers and bond midpoints), while the electronic polarizability of the protein is represented by dipole polarizability tensors for each

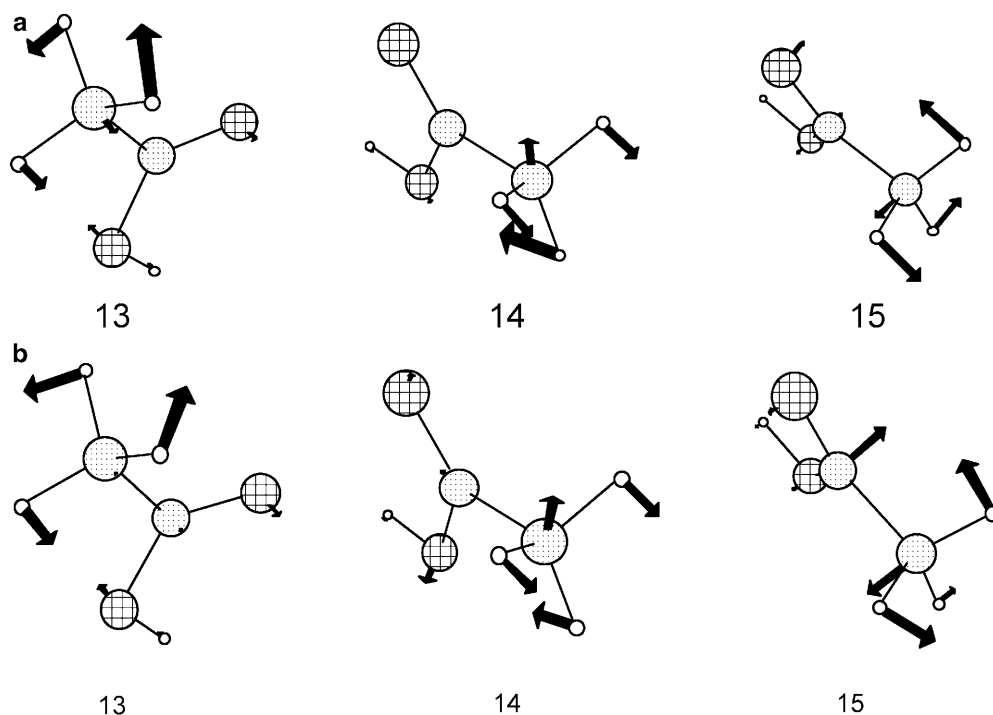


**Fig. 3.** **a** PHVA and **b** FHVA derived frequencies of acetic acid corresponding mainly to motion of the  $\text{CH}_3$  group relative to the  $\text{COOH}$  group (modes 13–15 in Table 1)

bond or lone-pair orbital [8]. Any covalent ab initio/EFP boundary is treated by a “buffer” region of frozen localized molecular orbitals [9] and, in the current implementation, the Cartesian coordinates of the EFP and buffer regions are kept fixed while the coordinates of the ab initio atoms are optimized.

Here we investigate the use of the PHVA in calculating the enthalpy and free-energy change due to deprotonation of the lysine  $\text{NH}_3^+$  group in the tripeptide GKG. The EFP/buffer/ab initio division (shown in Fig. 9) and the EFP and buffer construction are performed (at the RHF/MINI [10] level) as described in Ref. [8].<sup>2</sup>

Within the original EFP implementation, limited to noncovalent ab initio/EFP boundaries, each EFP has six degrees of freedom: rigid translation in the  $x$ ,  $y$ ,  $z$  direction and rigid rotation about the  $x$ ,  $y$ ,  $z$  component of the Cartesian unit vector originating at the EFP center of mass. Thus, there is no internal vibrational motion within an EFP, and in the GKG case (Fig. 12) the dimensions of  $\mathbf{K}_{\text{BB}}$  and  $\mathbf{K}_{\text{CC}}$  (Eq. 11) are 39 ( $3 \times 13$  ab initio atoms) and 21 ( $3 \times 5$  buffer atoms plus six EFP degrees of freedom), respectively.<sup>3</sup> The partial Hessian is constructed for both the protonated and deprotonated form of the lysine residue (where the ab initio region is optimized in each case) and used to compute  $\Delta H_{\text{trv}}$  and  $\Delta G_{\text{trv}}$ . These values are listed in Table 3, where they are compared to the FHVA and PHVA values calculated using an all ab initio description of GKG at completely optimized geometries.

<sup>2</sup>The MINI basis set is chosen for computational efficiency.

<sup>3</sup>The total mass of the EFP region is used to mass-weight these six Hessian components.

The all ab initio PHVA values are in error by less than 0.08–0.15 kcal/mol, which is consistent with the  $\alpha$ -amino tridecanoic acid results. The errors for the EFP values are only slightly larger (0.13–0.21 kcal/mol) and are certainly satisfactory.

The combined use of the PHVA and EFP methods thus provides a way of including (localized harmonic) free-energy changes for QM/MM simulations without performing molecular dynamics (MD) simulations. Indeed, Cui and Karplus [11] have developed a method by which a FHVA can be performed for a QM/MM energy function and have shown [12] that free energies derived from these harmonic frequencies yield free-energy barriers for an enzymatic reaction that agree well with experiment. Like any FHVA this necessitates a complete energy minimization of the system, which can be expensive for protein-sized systems (though, in general, much less expensive than a MD simulation). Future studies will address the degree to which global protein motion affects various experimental observables, such as barrier heights and  $\text{p}K_a$  values.

#### 4 Summary and conclusions

The PHVA used previously for the calculation of vibrational frequencies for adsorbates on surfaces [2] was extended to the calculation of vibrational enthalpy and entropy changes for chemical reactions in general. For deprotonation reactions, full HVA values were reproduced to within 0.1–0.4 kcal/mol, depending on the number of atoms included in the PHVA.

Similarly accurate results were obtained by the combined use of the PHVA and the hybrid EFP method [6]; thus, the PHVA method can provide (harmonic) free-

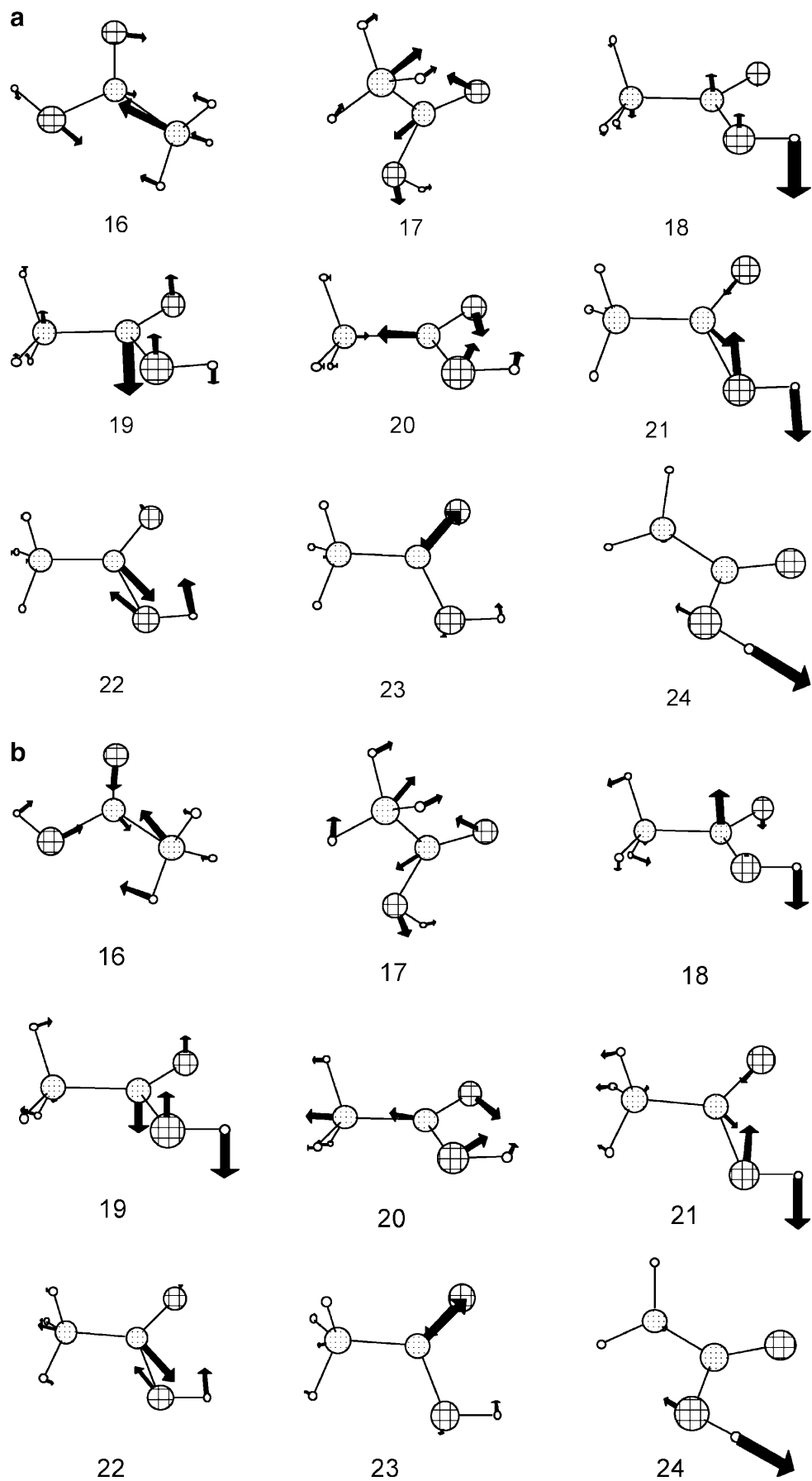


**Fig. 4. a** PHVA and **b** FHVA derived frequencies of acetic acid corresponding mainly to motion of the COOH group relative to the CH<sub>3</sub> group and internal motion of the COOH group (modes 16–24 in Table 1)

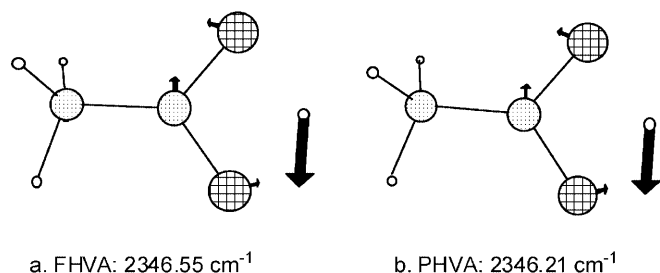


**Fig. 5.** The transition state and the corresponding imaginary frequency (a FHVA and b PHVA) of intramolecular proton transfer in acetic acid

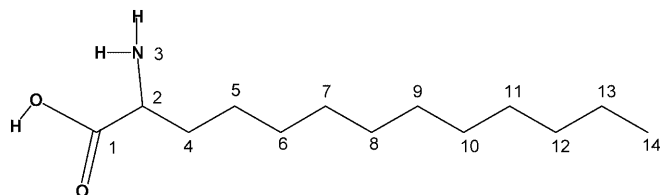


**Fig. 6.** Sketch of  $\alpha$ -amino tridecanoic acid (ATDA)

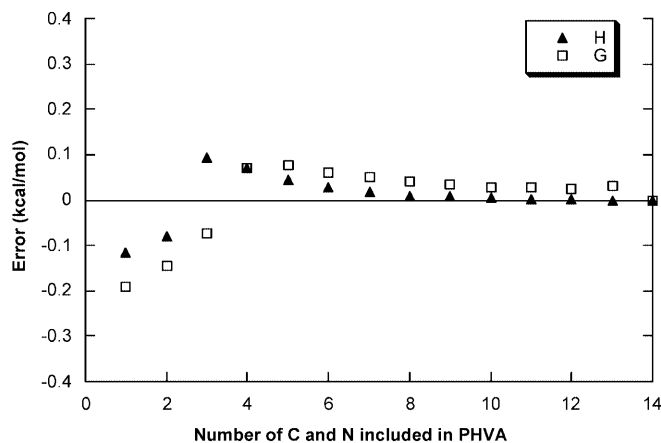


**Fig. 7.** Errors in the thermodynamic energy changes ( $\Delta H_{\text{trv}}$  and  $\Delta G_{\text{trv}}$ ) for deprotonation calculated by a PVHA relative to a FHVA for ATDA as a function of the number of CH<sub>2</sub> or NH<sub>2</sub> groups included in the PHVA (refer to Fig. 6 for numbering)

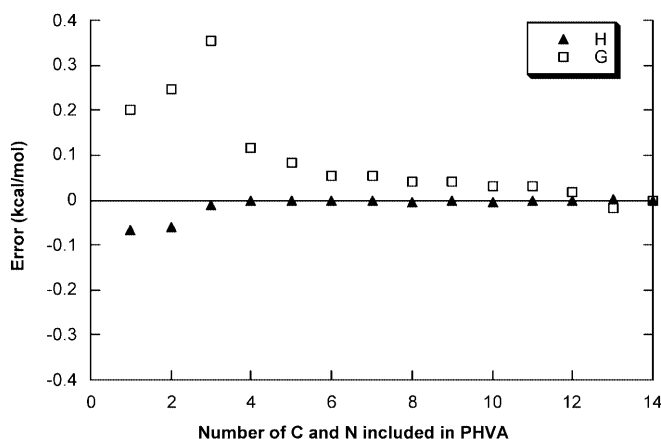


**Fig. 8.** Same as for Fig. 7 but for intramolecular proton transfer

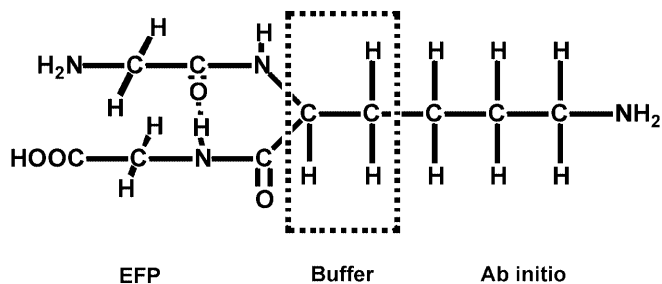


**Fig. 9.** Glycyl-lysyl-glycine tripeptide (deprotonated form) used for testing the PHVA within the effective fragment potential method

**Table 3.** Thermodynamical enthalpies ( $H_{\text{trv}}$ , kcal/mol) and entropies ( $G_{\text{trv}}$ , kcal/mol) of protonated (acid) and deprotonated (base) glycyl-lysyl-glycine tripeptide computed through the PHVA and the FHVA. The FHVA was done with full ab initio computation for all atoms (all ab initio FHVA). The PHVA was done both with full ab initio and effective fragment potential (EFP) methods. The energy change in the deprotonation process was calculated and the PHVA errors were compared to all ab initio FHVA

	All ab initio FHVA		All ab initio PHVA		EFP-PHVA	
	$H_{\text{trv}}$	$G_{\text{trv}}$	$H_{\text{trv}}$	$G_{\text{trv}}$	$H_{\text{trv}}$	$G_{\text{trv}}$
Acid	250.49	201.97	94.94	68.00	95.08	68.15
Base	242.02	193.81	86.39	59.69	86.48	59.78
$\Delta_{\text{base-acid}}$	-8.47	-8.16	-8.55	-8.31	-8.60	-8.37
$\Delta\Delta_{\text{PHVA-FHVA}}$			-0.08	-0.15	-0.13	-0.21

energy changes for localized chemical reactions in very large systems that are only partially optimized.

Finally, another, as yet untested but potentially very practical, application of the PHVA is the location of transition states. The usual approach is to construct a guess at the TS geometry, compute a Hessian to determine the number of imaginary frequencies, and then to proceed with the TS optimization using the Hessian, or to construct a new guess if the vibrational analysis shows no or too many large imaginary frequencies. The PHVA can be used to quickly check whether the guess geometry has a promising imaginary frequency. If so, a full Hessian can be calculated or the use of the partial Hessian in the optimization of the TS can be tried. Future studies will address this issue.

**Acknowledgements.** The authors thank Visvaldas Kairys and Frank Jensen for helpful discussions. This work was supported by a Research Innovation Award from the Research Corporation and a type G starter grant from the Petroleum Research Fund. H.L. gratefully acknowledges a predoctoral fellowship from the Center for Biocatalysis and Bioprocessing at the University of Iowa. The calculations were performed on IBM RS/6000 workstations obtained through a CRIF grant from the NSF (CHE-9974502).

## References

1. Pacchione G, Bagus PS, Parmigiani F (1992) Cluster models for surface and bulk phenomena. Plenum, New York

2. (a) Jin S, Head JD (1994) *Surf Sci* 318: 204; (b) Calvin MD, Head JD, Jin S (1996) *Surf Sci* 345: 161; (c) Head JD (1997) *Int J Quantum Chem* 65: 827–838; (d) Head JD, Shi Y (1999) *Int J Quantum Chem* 75: 815–820; (e) Head JD (2000) *Int J Quantum Chem* 77:350–357
3. Miller WH, Handy NC, Adams JE (1980) *J Chem Phys* 72: 99–112
4. Jensen F (1999) *Introduction to computational chemistry*. Wiley, New York, pp 296–307
5. Schmidt MW, Baldridge KK, Boatz JA, Elbert ST, Gordon MS, Jensen JH, Koseki S, Matsunaga N, Nguyen KA, Su S, Windus TL, Dupuis M, Montgomery JA (1993) *J Comput Chem* 14: 1347–1363
6. (a) Day PN, Jensen JH, Gordon MS, Webb SP, Stevens WJ, Kraus M, Garmer D, Basch H, Cohen D (1996) *J Chem Phys* 105: 1968–1986; (b) Gordon MS, Freitag M, Bandyopadhyay P, Jensen JH, Kairys V, Stevens WJ (2001) *J Phys Chem A* 105: 293–307
7. Stone AJ (1981) *Chem Phys Lett* 83:233–239
8. Minikis RM, Kairys V, Jensen JH (2001) *J Phys Chem A* 105: 293–307
9. Kairys V, Jensen JH (2000) *J Phys Chem A* 104: 6656–6665
10. Huzinaga S, Andzelm J, Klobukowski M, Radzio-Andzelm E, Sakai Y, Tatewaki H (1984) *Gaussian basis sets for molecular calculations*. Elsevier, Amsterdam
11. Cui Q, Karplus M (2000) *J Chem Phys* 112: 1133–1149
12. Cui Q, Karplus M (2001) *J Am Chem Soc* 123: 2284–2290